PAPER

Check for updates

Low-lying excited states of linear all-*trans* polyenes: the σ−π electron correlation and the description of ionic states†

Julio C. V. Chagas, [ID] ab Luan G. F. dos Santos, [ID] c Reed Nieman, [ID] c
Adelia J. A. Aquino, [ID] d Silmar A. do Monte, [ID] e Felix Plasser, [ID] f
Péter G. Szalay, [ID] g Hans Lischka [ID] *c and Francisco B. C. Machado [ID] *ab

In this work, the electronic spectra of all-*trans* polyenes, from hexatriene to dodecahexaene are investigated. Special attention is given to the challenging description of the ionic $1^1B_u^+$ state. A comprehensive wavefunction analysis of both singlet ($2^1A_g^-$, $1^1B_u^+$, and $2^1B_u^-$) and triplet excited states ($1^3A_g^-$ and $1^3B_u^-$) is performed using a range of multireference correlated methods, including multireference configuration interaction with singles and doubles (MR-CISD) including *a posteriori* size-extensivity Pople correction (+P), and the multireference averaged quadratic coupled-cluster (MR-AQCC) method. While covalent states are well described by multi-configurational self-consistent field (MCSCF) theory, accurately describing the ionic state requires addressing size-extensivity errors, basis set effects, and, most importantly, σ−π electron correlation. Taking these factors into account, MR-CISD+P and MR-AQCC results mutually corroborate that the ionic $1^1B_u^+$ state is the first vertically excited state in hexatriene and octatetraene. In decapentaene, extrapolated MR-CISD+P results indicate that the $2^1A_g^-$ and $1^1B_u^+$ states are nearly degenerate, while MR-AQCC suggests that the ionic state lies approximately 0.2 eV below the covalent state. From a wavefunction perspective, the ionic state is consistently well-represented by a single HOMO−LUMO excitation, whereas the contribution of doubly excited configurations increases with chain length for both covalent states.

1. Introduction

The study of linear all-*trans* polyenes has a long-standing tradition due to their distinctive spectral properties, which arise from the structure of their low-lying excited-state manifold. Polyenes serve as valuable models for chromophores in biological systems, such as carotenoids, which are crucial in photosynthetic processes. These processes include light-harvesting, particularly in the blue region of the visible spectrum,[1,2] and photoprotection through dissipation of excitation energy into heat.[3–5]

a Department of Chemistry, Aeronautics Institute of Technology, São José dos Campos 12228-900, Brazil. E-mail: fmachado@ita.br

b Advanced Scientific Computing and Modeling Laboratory, Aeronautics Institute of Technology, São José dos Campos 12228-900, Brazil

c Department of Chemistry and Biochemistry, Texas Tech University, Lubbock, TX 79409, USA. E-mail: hans.lischka@ttu.edu

d Department of Mechanical Engineering, Texas Tech University, Lubbock, TX 79409, USA

e Department of Chemistry, Federal University of Paraíba, João Pessoa 58051-900, Brazil

f Department of Chemistry, Loughborough University, Loughborough LE11 3TU, UK

g Institute of Chemistry, ELTE Eötvös Loránd University, Budapest H-1117, Hungary

† Electronic supplementary information (ESI) available. See DOI: https://doi.org/10.1039/d5cp00339c

Moreover, polyenes constitute a traditional set of molecules for testing theoretical concepts and benchmarking electronic structure methods,[6–16] thereby deepening the understanding of their electronic structure. Finally, various chromophores are built around polyene backbones inheriting their spectroscopic properties from the underlying polyene.[17,18] The three lowest excited states, in particular, have attracted significant attention both experimentally[19–23] and theoretically.[15,24–26] This study will focus on their description from an electronic structure perspective.

The electronic states of linear all-*trans* polyenes are conveniently identified using the irreducible representations of the C_{2h} symmetry associated with their molecular framework. Additionally, the states are labeled according to the nomenclature introduced by Pariser, which is based on the alternance symmetry derived from the Pariser–Parr–Pople[27–29] model Hamiltonian. In this approach, the linear combinations of the two degenerate transitions yield antisymmetric (−) and symmetric (+) states relative to the interchange of conjugated pairs of orbitals. In valence bond theory, these states are referred to as covalent (−) and ionic (+) states, respectively.[30] Notably, within the molecular orbital picture, distinguishing between ionic and covalent states is less straightforward.[31]

The relative ordering of the two low-lying excited singlet excited states, $2^1A_g^-$ and $1^1B_u^+$, in small all-*trans* linear polyenes, remains a topic of ongoing debate.[24] It is generally agreed that, for the first members of the series, the ionic $1^1B_u^+$ state is the first vertically excited state. As the chain length increases, the covalent $2^1A_g^-$ state becomes the lowest excited state. However, there is no consensus in the literature on the exact point in the series where this change occurs. A brief review of this aspect is provided in the following paragraphs. The $2^1A_g^-$ state exhibits high covalent character and has the same symmetry as the ground state; thus, the transition dipole moment between these two states vanishes entirely due to symmetry constraints, rendering this state strictly dark in one-photon absorption experiments. In contrast, the $1^1B_u^+$ state is a strongly optically allowed "bright" state with ionic character. The third vertically excited valence singlet excited state is the $2^1B_u^-$, which has a small transition dipole moment and exhibits covalent character.[25]

The wave functions of ionic states are primarily composed of singly excited configurations, whereas those of covalent states are more intricate, with significant contributions from doubly excited configurations.[32] This complexity is one of the main reasons why uniformly describing the electronic spectra of linear all-*trans* polyenes remains challenging from a theoretical perspective. Due to their nature, ionic states are relatively straightforward to describe using single-reference quantum chemical methods, such as time-dependent density functional theory (TD-DFT),[33–35] algebraic diagrammatic construction of second order (ADC(2)),[36] and equation of motion coupled-cluster (EOM-CCSD).[37] On the other hand, covalent states require the use of higher-level methods to capture static correlation effects effectively. Multiconfiguration self-consistent field (MCSCF) and multireference (MR) methods, in general, will be well suited for that purpose.

However, the MCSCF method and MR configuration interaction with singles and doubles (MR-CISD), which effectively capture static electron correlation effects and adequately describes covalent states, encounter notorious accuracy issues when applied to ionic states.[9,10,38] Specifically, excitation energies for ionic states are typically overestimated by about 1–2 eV when using an active space that includes only valence π-electrons and π-orbitals.[38] Several strategies have been proposed to mitigate this issue, such as expanding the active space to include additional unoccupied π-orbitals, including σ-orbitals into the active space, and modifying the one-electron basis set.[9,10,39–42] Indeed, a reasonable description of ionic states requires an extensive treatment of the σ–π electron correlation, which can in principle not be achieved by including correlation only in the π-space.[43]

Several methods have been employed to investigate the manifold of low-lying excited states in the series of all-*trans* polyenes. Here, we provide a brief review of key results. Hirao and co-workers,[44] using multireference Møller–Plesset (MRMP) theory, found that the $2^1A_g^-$ and $1^1B_u^+$ states are nearly degenerate in hexatriene. In longer polyenes, however, the covalent state becomes the first vertically excited state. This finding is corroborated by DFT/MRCI calculations performed by Marian

and Gilka,[14] which also show that the covalent state is the lowest singlet excited state in polyenes longer than hexatriene.

Serrano-Andrés and coworkers,[45,46] employing complete active space second-order perturbation theory (CASPT2), suggested that in terms of vertical excitation, the $1^1B_u^+$ state is the lowest excited state in hexatriene, lying 0.18 eV below the covalent state. In octatetraene, their results indicate that these states are virtually degenerate, with the $2^1A_g^-$ state being 0.04 eV lower than the $1^1B_u^+$ state. This trend is further supported by CASPT2 benchmark calculations.[47] The near-degeneracy of these two states in octatetraene is also corroborated by N-electron valence state second-order perturbation theory (NEVPT2) calculations.[41]

The most recent database of highly accurate excitation energies for electronic structures (QUESTDB),[48] which includes results based on coupled-cluster CCSDT and CC3 methods, suggests that the bright $1^1B_u^+$ state is the first vertically excited state in both hexatriene and octatetraene, being 0.25 eV and 0.12 eV lower than the covalent $2^1A_g^-$ state, respectively. This ordering is also obtained using CCSD and CC2 methods.[47]

MR-CISD,[43,49] and multireference averaged quadratic coupled-cluster (MR-AQCC)[50,51] calculations have been performed for ethylene[9] and butadiene,[10] the first members of the series. In the present work, we aim to achieve an accurate and balanced treatment of both static and dynamic electron correlation effects in all-*trans* linear polyenes, ranging from hexatriene up to dodecahexaene, using the variational MR-CISD and MR-AQCC methods. While nonvariational extensivity corrections are applied in the MR-CISD case, the MR-AQCC method inherently accounts for higher excitations, restoring size extensivity in an approximate yet considerably accurate manner.[52,53] We also seek to provide insights into the relative ordering of the excited states. A detailed analysis of the wave functions, based on the one-electron transition density matrix calculated with respect to the ground state, is presented. In particular, the ionic character of each state is assessed using the Q_a^t diagnostic, which has recently been shown to associate large transition charges centered on individual atoms with ionic states.[38] Complementary analysis of the one-electron transition density matrix provides insights into how the wave functions of the excited states evolve across the series in terms of multiconfigurational and single-excitation character.

2. Methods

2.1 Computational details

The equilibrium geometry of the ground state of linear all *trans*-polyenes containing N = 6, 8, 10, and 12 π-electrons (*trans,trans*-1,3,5-hexatriene, all-*trans*-1,3,5,7-octatetraene, all-*trans*-1,3,5,7,9-decapentaene, and all-*trans*-1,3,5,7,9,11-dodecahexaene, herein called hexatriene, octatetraene, decapentaene, and dodecahexaene, respectively) was obtained using the long-range corrected hybrid functional ω B97X-D[54] with the cc-pVTZ[55] basis set. Optimized geometries and analytical harmonic frequencies are available in the ESI.† Based on the optimized geometries, the

This journal is © the Owner Societies 2025

Phys. Chem. Chem. Phys., 2025, **27**, 7916–7928 | **7917**

singlet states $1^1A_g^-$, $2^1A_g^-$, $1^1B_u^+$, and $2^1B_u^-$, as well as the triplet excited states $1^3A_g^-$ and $1^3B_u^-$, were calculated at the multireference levels described below. Vertical excitation energies and oscillator strengths were computed for transitions between the ground state and the aforementioned states of interest. All calculations were performed strictly under C_{2h} symmetry constraints.

The ground and excited states were investigated using a range of computational methods, including state-averaged complete active space self-consistent field (SA-CASSCF) method,[56] MR-CISD,[43,49] and MR-AQCC[50,51] approaches. Where specified, the Pople (+P) correction,[57] extended to the MR-CISD case, was applied to account for size-extensivity errors. MR-AQCC calculations on excited states were conducted utilizing the vector-following approach in which convergence to a selected eigenvector was achieved using the criterion of maximal overlap with a specific root of the eigenvector of the reference space.

At the SA-CASSCF level, six states—namely $1^1A_g^-$, $2^1A_g^-$, $1^1B_u^+$, $2^1B_u^-$, $1^3A_g^-$, and $1^3B_u^-$—were averaged with equal weights. The resulting set of molecular orbitals was then used for subsequent MR-CISD and MR-AQCC calculations. SA-CASSCF computations were carried out with a standard valence active space, encompassing all valence π-electrons and valence π-orbitals of each molecule. To reduce the computational effort in the subsequent MR-CISD and MR-AQCC calculations, the reference space was constructed by splitting the π-valence space into three parts: a CAS(6,6), a complementary restrictive active space (RAS) for the remaining strongly occupied orbitals, and a corresponding auxiliary (AUX) space for weakly occupied orbitals of the π-valence space. Single excitations were used from RAS into CAS and AUX orbitals and from CAS into AUX orbitals. The specific choices used in our calculations are presented in Table 1. The restrictions imposed on the active space underwent extensive testing for decapentaene (Table S1, ESI†). The RAS(2)CAS(6,6)AUX(2) scheme, which contains ten π orbitals, closely reproduces the results obtained with the complete π-valence CAS(10,10). At both the MR-CISD and MR-AQCC levels, generalized interacting space restrictions[58] were applied.

For computational economy, a freezing scheme of σ-orbitals was employed at both the MR-CISD and MR-AQCC levels. After testing several freezing options for hexatriene (Table S2, ESI†), a scheme was adopted in which 50% of the reference doubly occupied σ-orbitals—including the core orbitals on each carbon atom, which constitute approximately 30% of the total reference doubly occupied σ-orbitals—and 50% of the reference virtual σ-orbitals were frozen. This freezing approach had no significant impact on excitation energies compared to the reference calculation, where only core orbitals were frozen (Table S2, ESI†).

The cc-pVnZ (n = D, T, Q) basis sets[55] were used with the outer shell of polarization functions excluded from the triple- and quadruple-ζ basis sets, as detailed below. Extrapolation to the complete basis set (CBS) limit was carried out using the two-point fit approach,[59] as shown in eqn (1) for the excitation energies obtained with the MR-CISD+P and MR-AQCC methods.

$$E_{XY}^{\infty} = \frac{E_X X^3 - E_Y Y^3}{X^3 - Y^3} \qquad (1)$$

In eqn (1), E_{XY}^{∞} represents the CBS limit excitation energy, X and Y are the cardinal numbers for the respective basis sets, and E_X and E_Y denote the excitation energies obtained for those individual basis sets. The cc-pVTZ basis set without the f-function, i.e., with contraction (10s,5p,2d)/[4s,3p,2d] (cc-pVTZ'), and the cc-pVQZ basis set without g-function, i.e., with contraction (12s,6p, 3d,2f)/[5s,4p,3d,2f] (cc-pVQZ') were used on carbon atoms for the basis set extrapolation to the CBS limit. The cc-pVDZ basis set was used on hydrogen in all cases.

Based on the optimized geometries, vertical excitation energies were also computed using second-order complete active space perturbation theory (CASPT2)[60] with the cc-pVDZ basis set. At the CASSCF level, singlet states of the same spatial symmetry were averaged with equal weights. The resulting set of molecular orbitals was used for subsequent CASPT2 computations, performed with IP-EA denominator shift 0.25. The SA-CASSCF and CASPT2 computations were performed with a standard valence CAS, including all valence π-electrons and π-orbitals of each molecule.

Geometry optimizations were carried out using the Gaussian 16 software package.[61] MR-CISD and MR-AQCC calculations were performed with the Columbus program system,[52,62,63] with integrals calculated by the Dalton program.[64] CASPT2 calculations were conducted using the OpenMolcas software package.[65]

2.2 Wavefunction descriptors

Based on the MR-CISD wavefunction, the ionic character of the excited states, the single-excitation character, and the participation ratio of natural transition orbitals (NTOs) were evaluated. To assess the ionic character of each state, the Q_a^t diagnostic[38] was employed, as defined in eqn (2),

$$Q_a^t = \sum_M |q_M^t| \qquad (2)$$

where the transition charge q_M^t on atom M is calculated as the sum over the diagonal elements of the one-electron transition density matrix (1TDM) between the states of interest and the ground state. Large transition charges centered on individual atoms are associated with ionic states. The Q_a^t values were computed based on the Löwdin-style population analysis.[66]

The participation ratio of natural transition orbitals (PR$_{NTO}$)[67,68] was used as a measure of the multiconfigurational

Table 1 Active reference space scheme utilized at the MR-CISD and MR-AQCC levels for polyenes with N π-electrons

N	Active space scheme
6	CAS(6,6)
8	RAS(1)CAS(6,6) AUX(1)
10	RAS(2)CAS(6,6) AUX(2)
12	RAS(3)CAS(6,6) AUX(3)

character of the excited states. The PR_{NTO} is computed as

$$PR_{NTO} = \frac{\left[\mathrm{tr}\left(\gamma_{0I}\gamma_{0I}^{T}\right)\right]^2}{\mathrm{tr}\left(\gamma_{0I}\gamma_{0I}^{T}\right)^2} \qquad (3)$$

where γ_{0I} is the 1TDM. PR_{NTO} counts how many different natural transition orbitals (NTOs) are participating and, thus, how many configurations are necessary to describe the excited state.

Finally, the single-excitation character, Ω, defined as $\Omega = \mathrm{tr}(\gamma_{0I}\gamma_{0I}^{T})$,[69,70] was calculated. Values above 0.8 computed based on correlated *ab initio* methods are indicative of singly excited states.[32,71] The three mentioned wavefunction descriptors were computed using the TheoDORE 3.1.1 program package.[72]

3. Results and discussion

3.1 Singlet states

We begin our discussion by presenting the vertical singlet excitation energy results. As previously mentioned, while covalent states are well-described by the CASSCF method, significant issues arise for the excitation energy from the ground state to the ionic $1^1B_u^+$ state. Using the cc-pVDZ basis set, CASSCF overestimates these excitation energies by 1.78 eV for hexatriene when compared to MR-CISD+P and MR-AQCC results (Table 2). This observation holds for the larger systems, with MR-AQCC tending to stabilize the ionic state slightly more than MR-CISD+P as the chain length increases. Overall, CASSCF overestimates the excitation energies by an average of 1.81 eV, ranging from 1.78 eV for hexatriene to 1.84 eV for dodecahexaene compared to MR-CISD+P results.

At the CASSCF level, the excitation energy to the ionic $1^1B_u^+$ state is not only higher than that of the $2^1A_g^-$ state but also exceeds that of the $2^1B_u^-$ state, causing the $1^1B_u^+$ state to become the second excited state of B_u symmetry. Notably, this inversion in the ordering of B_u symmetry states introduces additional challenges since, as discussed below, the ionic state in the systems studied here should be one of the two lowest-lying excited states when appropriate dynamic correlation is considered (Fig. 1). These artifacts of the CASSCF state ordering are significantly corrected at the MR-AQCC and MR-CISD+P levels, as Table 2 shows. The ionic $1^1B_u^+$ state is substantially stabilized compared to the CASSCF results. However, the use of a larger basis set appears to be particularly important for the ionic state. Therefore, a more detailed discussion of the state ordering is postponed to the respective discussion below.

Size-extensivity corrections play a significant role in describing the low-lying excited-state manifold in these systems. A closer inspection of Table 2, comparing uncorrected MR-CISD with MR-CISD+P values, reveals that the size-extensivity correction is more pronounced for the ionic state. This state is stabilized by values ranging from 0.58 eV for hexatriene to 0.70 eV for dodecahexaene, with stabilization consistently increasing as the system size grows (Table 2). Covalent states, on the other hand, are less affected by this correction. Specifically, the $2^1A_g^-$ state is stabilized by 0.04 eV in hexatriene and 0.23 eV in dodecahexaene. For the $2^1B_u^-$ state, the stabilization ranges from 0.07 eV for hexatriene to 0.35 eV for
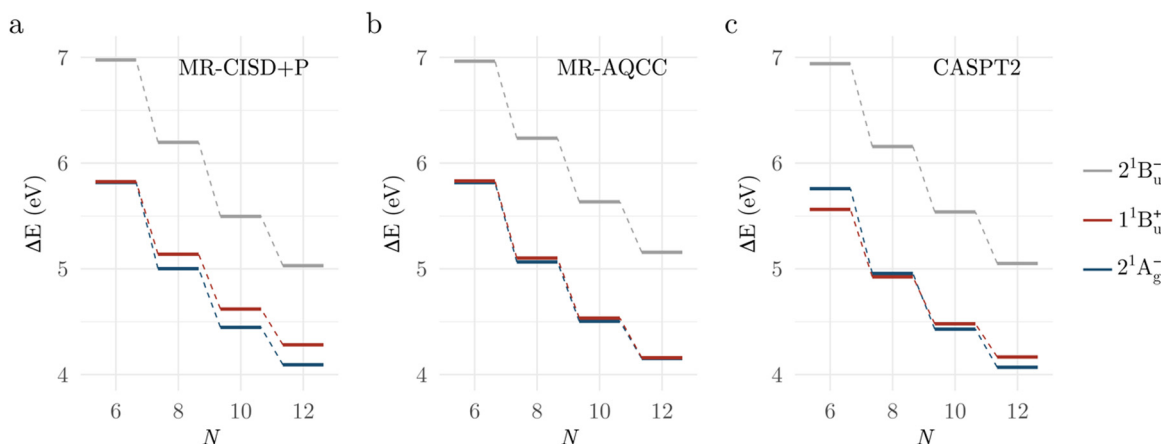
Table 2 Vertical singlet excitation energies of polyenes computed using the CASSCF, MR-CISD, MR-CISD+P, MR-AQCC, and CASPT2 methods and the cc-pVDZ basis set

		Method				
N	State	$CASSCF^a$	MR-CISD	MR-CISD+P	MR-AQCC	CASPT2
6	$2^1A_g^-$	5.799	5.856	5.819	5.818	5.761
	$1^1B_u^+$	7.609	6.412	5.827	5.833	5.564
	$2^1B_u^-$	6.983	7.044	6.976	6.964	6.941
8	$2^1A_g^-$	5.080	5.144	5.002	5.065	4.956
	$1^1B_u^+$	6.916	5.743	5.138	5.102	4.924
	$2^1B_u^-$	6.276	6.347	6.197	6.236	6.157
10	$2^1A_g^-$	4.598	4.648	4.448	4.505	4.431
	$1^1B_u^+$	6.448	5.311	4.622	4.536	4.482
	$2^1B_u^-$	5.673	5.838	5.498	5.636	5.540
12	$2^1A_g^-$	4.268	4.323	4.093	4.153	4.069
	$1^1B_u^+$	6.123	4.978	4.282	4.160	4.167
	$2^1B_u^-$	5.216	5.377	5.030	5.157	5.052

^{a} The B_u states are numbered according to wave function character, not by energetic order.

Fig. 1 Vertical singlet excitation energies of polyenes with N π-electrons computed using (a) MR–CISD+P, (b) MR-AQCC, and (c) CASPT2. Calculations were performed with the cc-pVDZ basis set. Numerical data are available in Table 2.

Table 3 Singlet excitation energies (eV) of polyenes with N π-electrons, calculated at the MR-CISD+P and MR-AQCC levels using the cc-pVDZ ($\Delta E_{\text{cc-pVDZ}}$), cc-pVTZ′ ($\Delta E_{\text{cc-pVTZ}'}$), and cc-pVQZ′ ($\Delta E_{\text{cc-pVQZ}'}$) basis sets

		MR-CISD+P			MR-AQCC		
N	State	$\Delta E_{\text{cc-pVDZ}}$	$\Delta E_{\text{cc-pVTZ}'}$	$\Delta E_{\text{cc-pVQZ}'}$	$\Delta E_{\text{cc-pVDZ}}$	$\Delta E_{\text{cc-pVTZ}'}$	$\Delta E_{\text{cc-pVQZ}'}$
6	$2^1A_g^-$	5.819	5.793	5.776	5.818	5.783	5.755
	$1^1B_u^+$	5.827	5.638	5.584	5.833	5.620	5.504
	$2^1B_u^-$	6.976	6.907	6.895	6.964	6.813	6.648
8	$2^1A_g^-$	5.002	4.984	4.988	5.065	5.036	5.025
	$1^1B_u^+$	5.138	4.975	4.941	5.102	4.904	4.804
	$2^1B_u^-$	6.197	6.168	6.180	6.236	6.152	6.079
10	$2^1A_g^-$	4.448	4.427	—	4.505	4.465	—
	$1^1B_u^+$	4.622	4.480	—	4.536	4.332	—
	$2^1B_u^-$	5.498	5.479	—	5.636	5.549	—
12	$2^1A_g^-$	4.093	4.026[a]	—	4.153	4.084[a]	—
	$1^1B_u^+$	4.282	4.139[a]	—	4.160	3.962[a]	—
	$2^1B_u^-$	5.030	5.075[a]	—	5.157	5.189[a]	—

[a] Estimated result based on a fit of excitation energies across the series (Fig. S4, ESI).

dodecahexaene (Table 2). These results are depicted graphically in Fig. S1 (ESI†).

To assess the influence of the basis set on the excitation energies and to discuss the relative ordering of the two low-lying excited states across the series, extrapolation to the complete basis set (CBS) limit was performed using the two-point fit approach (eqn (1)) based on MR-CISD+P and MR-AQCC calculations. The results obtained with the cc-pVDZ, cc-pVTZ′, and cc-pVQZ′ basis sets are presented in Table 3 for MR-CISD+P and MR-AQCC. The extrapolated values, derived from the double- to

Table 4 MR-CISD+P and MR-AQCC vertical singlet excitation energies (in eV) of polyenes with N π-electrons at the CBS limit. Values were computed by extrapolating from the double-ζ cc-pVDZ to the triple-ζ cc-pVTZ′ (DT) and from the triple-ζ cc-pVTZ′ to the quadruple-ζ cc-pVQZ′ (TQ). Reference theoretical values are provided for comparison

		MR-CISD+P		MR-AQCC			
N	State	$\Delta E_{\text{DT}}^{\infty}$	$\Delta E_{\text{TQ}}^{\infty}$	$\Delta E_{\text{DT}}^{\infty}$	$\Delta E_{\text{TQ}}^{\infty}$	TBE[b]	CASPT2
6	$2^1A_g^-$	5.781	5.765	5.768	5.734	5.62[c]	5.57[e]
	$1^1B_u^+$	5.559	5.543	5.530	5.420	5.37[c]	5.31[f]
	$2^1B_u^-$	6.879	6.886	6.749	6.528	—	—
8	$2^1A_g^-$	4.977	4.991	5.025	5.016	4.90[d]	4.74[e]
	$1^1B_u^+$	4.906	4.917	4.820	4.731	4.78[d]	4.70[f]
	$2^1B_u^-$	6.156	6.188	6.117	6.026	—	—
10	$2^1A_g^-$	4.418	—	4.449	—	—	—
	$1^1B_u^+$	4.420	—	4.246	—	—	—
	$2^1B_u^-$	5.471	—	5.513	—	—	—
12	$2^1A_g^-$	4.019[a]	—	4.070[a]	—	—	—
	$1^1B_u^+$	4.080[a]	—	3.883[a]	—	—	—
	$2^1B_u^-$	5.082[a]	—	5.166[a]	—	—	—

[a] Estimated result based on a fit of excitation energies across the series (Fig. S5, ESI). [b] Theoretical best estimates (TBE) collected from ref. 48, computed as "A/SB + [B/TB − B/SB]," where A/SB is the excitation energy computed with a method A in a smaller basis (SB), and B/SB and B/TB are excitation energies computed with a method B in the small basis and target basis TB, respectively. [c] CCSDT/AVDZ + [CC3/AVTZ-CC3/AVDZ]. [d] CCSDT/6-31+G(d) + [CC3/AVTZ-CC3/6-31+G(d)]. [e] Collected from ref.73 aug-cc-pVTZ basis set. [f] Collected from ref. 47 TZVP basis set.
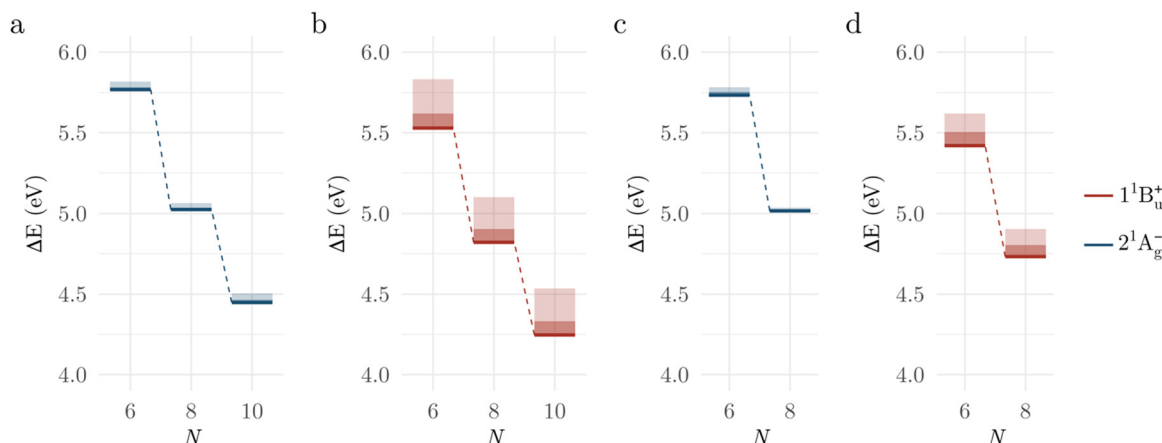
triple-ζ basis set ($\Delta E_{\text{DT}}^{\infty}$) and the triple- to quadruple-ζ basis set ($\Delta E_{\text{TQ}}^{\infty}$) extrapolation, are summarized in Table 4.

The first major observation is that the two low-lying excited states are affected differently when additional polarization functions are added to the basis set (Table 3). Let us first consider expanding the basis set from double- to triple-ζ. For hexatriene, the $2^1A_g^-$ state is stabilized by 0.03 eV, whereas the ionic state is stabilized by approximately 0.2 eV based on MR-AQCC results—a similar trend is observed with MR-CISD+P results. For octatetraene and decapentaene, at the MR-AQCC level, a similar trend is seen: the covalent state is stabilized by about 0.03–0.04 eV, while the ionic state is stabilized by about 0.2 eV. On the other hand, for the results obtained at the MR-CISD+P level, the behavior changes slightly as the chain length increases. While the covalent state is still stabilized by 0.02–0.03 eV, in agreement with MR-AQCC results, the stabilization of the ionic state decreases slightly with chain length, specifically, by 0.19 eV, 0.16 eV, and 0.14 eV in hexatriene, octatetraene, and decapentaene, respectively.

For dodecahexaene, computational cost constraints prevented the use of basis sets larger than the double-ζ cc-pVDZ. However, a crude estimate for the excitation energies using the cc-pVTZ′ basis set was made for $N = 12$ using a power function fit (see Section 2.1 of the ESI†). This estimate suggests that these trends hold for dodecahexaene. While the covalent state is stabilized by 0.07 eV at both the MR-AQCC and MR-CISD+P levels, the ionic state is stabilized by 0.2 eV at the MR-AQCC level and by 0.14 eV at the MR-CISD+P level. It is worth noting that, while the stabilization of the ionic state is consistent with what is observed for the smaller members of the series at both levels, the stabilization predicted for the covalent state is larger than the 0.02–0.03 eV observed for the smaller members of the series when expanding the basis set from double- to triple-ζ.

Using the cc-pVTZ basis set, our MR-AQCC results indicate that the ionic state is the first vertically excited state in hexatriene, octatetraene, decapentaene, and dodecahexaene, lying 0.16 eV, 0.13 eV, 0.13 eV, and 0.12 eV below the covalent $2^1A_g^-$ state, respectively. In contrast, MR-CISD+P results suggest that the ionic state is the first vertically excited state in hexatriene, that the two low-lying excited states are nearly degenerate in octatetraene, and that the covalent $2^1A_g^-$ state lies below the ionic state by 0.05 eV in decapentaene and by 0.11 eV in dodecahexaene.

When comparing triple-ζ and quadruple-ζ basis set results, as expected, the stabilization effect is smaller than when expanding from the double- to triple-ζ basis set. For hexatriene, at the MR-AQCC level, the covalent state is stabilized by about 0.03 eV, while the ionic state is stabilized by approximately 0.12 eV. At the MR-CISD+P level, the covalent state is stabilized by 0.02 eV and the ionic state by 0.05 eV. For octatetraene, the covalent state shows a negligible effect from basis set expansion at both the MR-AQCC and MR-CISD+P levels. The ionic state, on the other hand, is further stabilized: by 0.10 eV at the MR-AQCC level, and by 0.03 eV at the MR-CISD+P level.

Using the cc-pVQZ basis set, MR-AQCC results show that the ionic state is the first vertically excited state in hexatriene and

Fig. 2 Vertical singlet excitation energies of polyenes with N π-electrons, obtained by extrapolating MR-AQCC results to the complete basis set limit using (a), (b) DT and (c), (d) TQ extrapolations. The height of the lighter shaded bar indicates the difference between excitation energies obtained with the smaller and larger basis sets. The height of the darker shaded bar represents the difference between the larger basis set result and the extrapolated CBS value (represented by the marker).

octatetraene, lying 0.25 eV and 0.22 eV below the covalent $2^1A_g^-$ state, respectively. MR-CISD+P results indicate the same ordering, with a splitting between the two low-lying excited states of 0.19 eV and 0.05 eV in hexatriene and octatetraene, respectively. The results obtained for the different basis sets are shown graphically in Fig. 2 for MR-AQCC and in Fig. S2 (ESI†) for MR-CISD+P.

Benchmark theoretical vertical excitation energy values are available for hexatriene and octatetraene (Table 4). In addition to data from the QUESTDB database of highly accurate excitation energies,[48] reference CASPT2 results for the ionic state were collected from the benchmark for electronically excited states in ref. 47, whereas CASPT2 results for the covalent state were taken from the reference energies for double excitations collection in ref. 73 All collected reference values were computed using triple-ζ basis sets.

For hexatriene, the theoretical best estimates (TBE) from the QUESTDB database[48] predict the ionic state to lie 0.25 eV below the covalent $2^1A_g^-$ state (Table 4). This aligns with the reference CASPT2 values, which predict the ionic state to lie 0.26 eV below the covalent state. The ΔE_{DT}^∞ extrapolated excitation energies based on MR-AQCC results suggest the ionic state lies 0.24 eV below the covalent state, while the equivalent value based on MR-CISD+P computation is 0.22 eV. For the ΔE_{TQ}^∞ extrapolated values, the relative differences between the two low-lying states are 0.31 eV at the MR-AQCC level and 0.22 eV at the MR-CISD+P level, with the ionic state being the first vertically excited state. The agreement between the reference theoretical values and our extrapolated results provides strong evidence that the ionic state is the first vertically excited state in hexatriene.

For octatetraene, data from the QUESTDB database indicate that the ionic state lies 0.12 eV below the covalent $2^1A_g^-$ state (Table 4). The reference CASPT2 results suggest that these states are nearly degenerate, with the ionic state lying only 0.04 eV below the covalent state, a difference within chemical accuracy. The ΔE_{DT}^∞ extrapolated excitation energies based on

MR-AQCC and MR-CISD+P results suggest that the ionic state lies below the covalent state by 0.21 eV and 0.07 eV, respectively. The ΔE_{TQ}^∞ extrapolated values show the same trend as the ΔE_{DT}^∞ extrapolated values, with relative differences between the two states of 0.29 eV at the MR-AQCC level and 0.07 eV at the MR-CISD+P level. Our MR-AQCC results suggest that the $1^1B_u^+$ state is the first vertically excited state in octatetraene, whereas MR-CISD+P, while suggesting the same ordering, shows a splitting of only 0.07 eV between the two low-lying excited states.

For decapentaene, excitation energies were obtained using double- and triple-ζ basis sets. Calculations with a quadruple-ζ basis set were not feasible, precluding a more reliable ΔE_{TQ}^∞ extrapolation. Based on ΔE_{DT}^∞ values, MR-AQCC results indicate that the ionic state remains lower than the covalent $2^1A_g^-$ state by approximately 0.20 eV (Table 4). MR-CISD+P results predict that the $2^1A_g^-$ and $1^1B_u^+$ states are virtually degenerate, with the splitting between the two states within chemical accuracy.

For dodecahexaene, the computational cost associated with using basis sets larger than the double-ζ cc-pVDZ prevented an accurate assignment of the relative ordering of the two low-lying excited states. However, a crude estimate for the ΔE_{DT}^∞ extrapolated results made for $N = 12$ using a power function fit (Fig. S5, ESI†) indicates that, at the MR-AQCC level, the ionic state is the first vertically excited state, lying 0.19 eV below the covalent $2^1A_g^-$ state. The MR-CISD+P estimates suggest that the covalent $2^1A_g^-$ state is the first vertically excited state, lying 0.06 eV below the ionic state.

The results in Table 4 incorporate all relevant effects necessary for accurately describing both the ionic and covalent states, including σ-electron correlation, size-extensivity correction, and basis set effects. Thus, these results represent a comprehensive and well-balanced description of vertical excitation energies. In summary, compared to excitation energies obtained at the MR-AQCC and MR-CISD+P levels using the cc-pVDZ basis set (Table 2), the significant stabilization of the ionic state relative to the covalent $2^1A_g^-$ state—caused by

This journal is © the Owner Societies 2025

Phys. Chem. Chem. Phys., 2025, **27**, 7916–7928 | **7921**

including larger shells of polarization functions—leads to the $1^1B_u^+$ state becoming the first vertically excited state in hexatriene and octatetraene. This state ordering, obtained at both the MR-AQCC and MR-CISD+P levels, agrees well with the reference TBE and CASPT2 values (Table 4). Extrapolated MR-AQCC results show somewhat better numerical agreement with the aforementioned reference data. Beyond octatetraene (Table 4), MR-AQCC consistently stabilizes the ionic state further, which remains slightly lower in energy than the covalent state for the polyene sizes investigated here. Extrapolated MR-CISD+P results (Table 4) suggest a slightly different picture, as they stabilize the ionic state less. The two lowest excited states are virtually degenerate in decapentaene, with the covalent $2^1A_g^-$ state being the first vertically excited state in longer polyenes. The extrapolated results are shown graphically in Fig. 2 for MR-AQCC calculations and Fig. S2 (ESI†) for MR-CISD+P calculations.

The accuracy of experimental estimates for vertical excitation energies varies significantly between the $1^1B_u^+$ and $2^1A_g^-$ states due to their differing accessibility in one-photon processes. The $1^1B_u^+$ state is easily observed in one-photon absorption experiments, whereas the $2^1A_g^-$ state is optically dark, requiring more sophisticated detection techniques. Experimental estimates for the excitation energies for the $2^1A_g^-$ state have been extensively debated in the literature.[26,41,46] These estimates are made using the mirror-image symmetry rule, which assumes that the energy difference between the (0–0) and vertical excitation energies is equal to the difference between the (0–0) and fluorescence intensity maximum—i.e., vertical excitation energies are estimated as (0–0) + [(0–0) – fluorescence intensity maximum]. However, this approximation is valid only under the assumption that the potential energy surfaces of the $1^1A_g^-$ and $2^1A_g^-$ states are sufficiently similar—a condition that is not necessarily true for polyenes. Indeed, theoretical studies show that this approach can significantly underestimate the excitation energy due to substantial differences in the potential energy surfaces of the electronic states involved.[44,74]

On the other hand, the experimental vertical excitation energy to the ionic $1^1B_u^+$ state is typically estimated from the absorption spectrum, where the maximum of the absorption band associated with the $1^1B_u^+ \leftarrow 1^1A_g^-$ excitation—which, in this case, also represents the origin peak—is often compared with theoretical vertical excitation energies. However, it has been previously demonstrated that vertical excitation energies at the ground-state minimum are blue-shifted relative to the band maximum by about 0.2 eV.[75] For hexatriene and octatetraene, gas-phase spectra or high-resolution spectra of the jet-cooled compound are available,[21,22,76–80] whereas for decapentaene and dodecahexaene fewer experimental data are available. An extrapolation to the gas phase from the origins of the two lowest-lying excited states measured in the condensed phase was carried out by D'Amico and coworkers for decapentaene and dodecahexaene.[23] This extrapolation has been shown to be in good agreement with gas-phase data for decapentaene.[23]

Experimental gas-phase estimates for vertical singlet excitation energies of linear all-*trans* polyenes are presented in Table 5. For hexatriene, when comparing the experimental

estimates for the $1^1B_u^+$ state with the ΔE_{TQ}^∞ extrapolated results obtained at the MR-AQCC level (Table 4)—which best match the reference theoretical values—our calculated vertical excitation energy for the ionic state in hexatriene is 0.49 eV higher than the experimental estimate. The reference TBE from QUESTDB is 0.44 eV higher, while the reference CASPT2 result is 0.38 eV higher than the experimental estimate. These reference theoretical values are in good agreement with our findings. Taking into account that vertical excitation energies are estimated to be around 0.2 eV higher than the experimental band maximum,[75] our calculated values also show good agreement with the experimental estimate.

In octatetraene, our ΔE_{TQ}^∞ extrapolated MR-AQCC results for the $1^1B_u^+$ state suggest a vertical excitation energy that is 0.32 eV higher than the experimental band maximum (Tables 4 and 5). The reference TBE from QUESTDB is 0.37 eV higher, while the CASPT2 result is 0.29 eV higher than the experimental estimate. Again, these findings are consistent with our results and are in good agreement with the experimental estimate, assuming, as before, that vertical excitation energies are blue-shifted relative to the band maximum by about 0.2 eV.[75] For the vertical excitation energy to the covalent $2^1A_g^-$ state, the ΔE_{TQ}^∞ extrapolated results indicate that the experimental estimate based on the mirror-image symmetry rule underestimates the vertical excitation energy by 0.94 eV. This underestimation is 0.82 eV based on the QUESTDB reference, and 0.66 eV based on the CASPT2 reference result.

In decapentaene, ΔE_{DT}^∞ extrapolated MR-AQCC results predict that the vertical excitation energy for the $1^1B_u^+$ state is 0.27 eV higher than the band maximum (Tables 4 and 5). For the $2^1A_g^-$ state, the extrapolated result suggests that the experimental estimate based on the mirror-image symmetry rule underestimates the vertical excitation energy by 0.97 eV, consistent with what was observed for octatetraene.

In dodecahexaene, based on our estimate for the ΔE_{DT}^∞ extrapolated MR-AQCC results (Table 4), the vertical excitation

Table 5 Experimental estimates for gas-phase vertical excitation energies (eV) for the two lowest excited singlet states of polyenes with N π-electrons

N	State	Experimental data
6	$2^1A_g^-$	—
	$1^1B_u^+$	4.93^a, 4.93^b
8	$2^1A_g^-$	4.08^c
	$1^1B_u^+$	4.41^d, 4.41^e
10	$2^1A_g^-$	3.48^f
	$1^1B_u^+$	3.98^g
12	$2^1A_g^-$	2.91^f
	$1^1B_u^+$	3.65^g

^{a} Absorption band maximum.[21] ^{b} Absorption band maximum of the jet-cooled compound.[78] ^{c} Estimated assuming mirror symmetry between absorption and emission.[80] ^{d} Absorption band maximum of the jet-cooled compound.[77] ^{e} Absorption band maximum of the jet-cooled compound.[79] ^{f} Estimated assuming mirror symmetry between absorption and emission. Vibronic patterns for the gas and condensed phases are assumed to be similar.[23] ^{g} Absorption band maximum in the condensed phase. Extrapolated to gas phase using solvent shift theory.[23]

7922 | *Phys. Chem. Chem. Phys.*, 2025, **27**, 7916–7928

This journal is © the Owner Societies 2025

energy for the $1^1B_u^+$ state is predicted to be 0.23 eV higher than the band maximum (Tables 1 and 5). Our results for the covalent $2^1A_g^-$ state suggest that the experimental estimate based on the mirror-image symmetry rule underestimates the vertical excitation energy by 1.16 eV, in agreement with what was observed for the smaller members of the series.

3.2 Triplet states

The two lowest triplet states-$1^3A_g^-$ and $1^3B_u^-$-are covalent states. Similar to the singlet covalent states, these triplet states are well-described without the need for extensive dynamic correlation treatments. Considering all the polyenes studied, SA-CASSCF results exhibit an average difference of 0.08 eV for the $1^3A_g^-$ state and 0.04 eV for the $1^3B_u^-$ state compared to MR-CISD+P values (Table 6). When compared to MR-AQCC results, the average differences are 0.08 eV and 0.05 eV for the $1^3A_g^-$ and $1^3B_u^-$ states, respectively.

The differences between MR-CISD+P, MR-AQCC, and CASPT2 results for both the $1^3A_g^-$ and $1^3B_u^-$ states do not exceed 0.05 eV (Table 6). This indicates that these triplet states are reliably calculated using these methods. The CASSCF results are in close agreement with those obtained using MR-CISD+P, MR-AQCC, and CASPT2 (Table 6), suggesting that σ–π electron correlation does not significantly impact the description of these states. The primary exception is the excitation energy to the $1^3A_g^-$ state of hexatriene, where the CASSCF result underestimates the energy by approximately 0.18 eV compared to MR-CISD+P and MR-AQCC.

Size-extensivity corrections also have no significant effect on the vertical excitation energies of the $1^3A_g^-$ and $1^3B_u^-$ states for the systems studied. The MR-CISD results are not significantly different from the size-extensivity-corrected MR-CISD+P values (Table 6). Likewise, the addition of polarization functions to the basis set does not substantially change the vertical excitation energies for these states when using either the MR-CISD+P (Table S3, ESI†) or MR-AQCC (Table S4, ESI†) methods.

Experimental data for hexatriene and octatetraene are available from low-energy electron impact spectra and electron energy loss spectra, respectively (Table 7). In comparison with MR-AQCC results for hexatriene (Table 6), the calculated results predict excitation energies that are 0.34 eV and 0.49 eV higher

Table 7 Experimental estimates for gas-phase vertical excitation energies (eV) for the two lowest triplet states of polyenes with N π-electrons

N	State	Experimental data
6	$1^3B_u^-$	2.61^a
	$1^3A_g^-$	4.11^a
8	$1^3B_u^-$	2.10^b
	$1^3A_g^-$	3.55^b

[a] Band maximum of low-energy electron impact spectrum.[81] [b] Band maximum of electron energy-loss spectrum.[82]

than the band maximum for the $1^3B_u^-$ and $1^3A_g^-$ states, respectively. For octatetraene, the MR-AQCC results suggest that the excitation energies are 0.46 eV and 0.38 eV higher than the band maximum of the electron energy loss spectrum for the $1^3B_u^-$ and $1^3A_g^-$ states, respectively.

3.3 Wavefunction analysis

We now shift our focus to analyzing the wave functions of the polyenes, with particular emphasis on the singlet states. Fig. S3–S6 (ESI†) illustrate the hole and electron natural transition orbitals (NTOs) computed at the MR-CISD level for each system. The transition densities for the excited states $2^1A_g^-$, $1^1B_u^+$, and $2^1B_u^-$ of hexatriene, calculated with respect to the ground state, are shown in Fig. 3. Transition densities for all the systems are depicted in Fig. S7 (ESI†).

Examination of the transition density (Fig. 3) shows that for covalent states, the transition densities are centered along the bonds, while for the ionic state, they are localized on the atoms. In covalent states, transition density contributions from either side of an atom tend to cancel out, resulting in a net zero transition charge q_M^t (transition charge values are available in Section S5 of ESI†). In contrast, ionic states exhibit non-vanishing transition charges on individual atoms. Moreover, the importance of σ–π electron correlation is evident not only in the excitation energies but also in the transition densities. The transition density of the ionic state at the MR-CISD level shows distinct σ-contributions that are absent in the CASSCF transition density. This observation holds consistently across all polyenes investigated.

These σ-contributions are associated with the reduction of transition density self-repulsion. Self-repulsion is generally large when there is significant spatial overlap between the involved orbitals and becomes smaller when the orbitals are spatially separated.[31,71,83–85] The role of transition density self-repulsion has been investigated by Kimber and Plasser.[31,71,85] Their works demonstrate that, while the self-repulsion term raises the excitation energy, it can be compensated by σσ* excitations. Consequently, the inclusion of σ-contributions in the wavefunction reduces the energetic penalty of the pure HOMO–LUMO transition,[38] lowering the excitation energy and resulting in reduced oscillator strengths, as observed in MR-CISD calculations compared to CASSCF results (Table S5, ESI†).

As anticipated, progressively reducing the degree of σ–π electron correlation by freezing σ-orbitals at the CI step has noticeable effects on transition densities (Fig. 4(a)) and

Table 6 Vertical triplet excitation energies of polyenes with N π-electrons computed using CASSCF, MR-CISD, MR-CISD+P, MR-AQCC, and CASPT2 methods. Calculations were performed with the cc-pVDZ basis set

N	State	Method				
		CASSCF	MR-CISD	MR-CISD+P	MR-AQCC	CASPT2
6	$1^3B_u^-$	2.860	2.940	2.948	2.945	2.941
	$1^3A_g^-$	4.421	4.574	4.608	4.598	4.553
8	$1^3B_u^-$	2.539	2.563	2.581	2.562	2.569
	$1^3A_g^-$	3.845	3.931	3.933	3.928	3.925
10	$1^3B_u^-$	2.330	2.321	2.330	2.294	2.335
	$1^3A_g^-$	3.429	3.502	3.465	3.466	3.466
12	$1^3B_u^-$	2.193	2.169	2.182	2.137	2.178
	$1^3A_g^-$	3.121	3.182	3.116	3.121	3.140

This journal is © the Owner Societies 2025

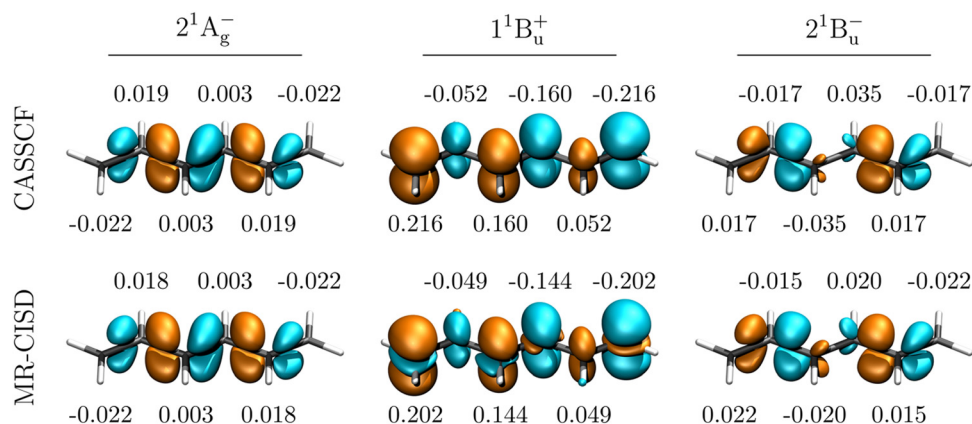*Phys. Chem. Chem. Phys.*, 2025, **27**, 7916–7928 | **7923**

Fig. 3 Transition densities (isovalue: ±0.002 a.u.) between the ground state and the excited states $2^1A_g^-$, $1^1B_u^+$, and $2^1B_u^-$ of hexatriene, computed at the CASSCF and MR-CISD levels of theory. Transition charges on carbon atoms are displayed.

excitation energies (Fig. 4(b)). Freezing 50% of reference doubly occupied σ-orbitals and 50% of reference virtual σ-orbitals has minimal impact on the excitation energies or transition densities. However, as the percentage of frozen σ-orbitals increases, the σ-contributions in the transition densities vanish, the excitation energies increase, and size-extensivity corrections become less effective.

Lastly, we examine the evolution of the wavefunction across the polyene series in terms of ionic character (Q_t^a), multiconfigurational character (PR_{NTO}), and single-excitation character

(Ω). The results for these descriptors are summarized in Table 8.

The results in Table 8 suggest that the descriptors for excitation to the ionic state change only slightly across the polyene series. The Q_t^a values effectively distinguish the ionic state from the covalent states by indicating significant transition charges localized on individual atoms, as has been observed in other systems.[38] Additionally, the NTO participation ratio (PR_{NTO}) shows that the ionic state is predominantly described by a single pair of hole and electron NTOs, which is consistent with the fact that these are predominant HOMO–LUMO transitions. The single-excitation character (Ω), with values higher than 0.8, emphasizes its singly-excited nature with only minor correlation contributions.

In contrast, the covalent states exhibit more pronounced changes in their wavefunction descriptors throughout the series. The multiconfigurational character of the $2^1A_g^-$ state remains nearly constant, while for the $2^1B_u^-$ state it increases slightly as the chain lengthens. Regarding the single-excitation character Ω, we note that this value is below 0.5 for both covalent states of all molecules investigated, highlighting that these states possess more than 50% double excitation character. In addition, we note that the single-excitation character slightly decreases suggesting that the contribution of
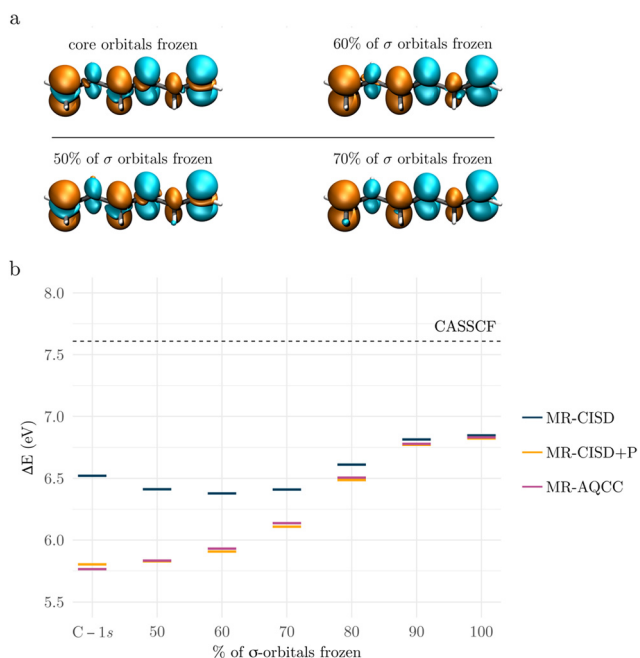

Fig. 4 Influence of freezing σ-orbitals in hexatriene on (a) transition densities (isovalue: ±0.002 a.u.) between the ground state and the $1^1B_u^+$ state, and (b) excitation energies computed at the MR-CISD level with the cc-pVDZ basis set. The percentage of σ-orbitals refers to the percentage of reference doubly occupied σ-orbitals and the corresponding percentage of reference virtual σ-orbitals frozen. C-1s indicates that only carbon core orbitals were frozen.

Table 8 Characterization of excited states based on ionic character Q_t^a, single-excitation character Ω, and NTO participation ratio PR_{NTO} calculated from the MR-CISD wave function

N	State	Q_t^a	PR_{NTO}	Ω
6	$2^1A_g^-$	0.089	1.994	0.404
	$1^1B_u^+$	0.872	1.087	0.871
	$2^1B_u^-$	0.117	1.994	0.468
8	$2^1A_g^-$	0.090	2.029	0.368
	$1^1B_u^+$	0.879	1.101	0.854
	$2^1B_u^-$	0.148	2.158	0.402
10	$2^1A_g^-$	0.078	2.062	0.344
	$1^1B_u^+$	0.889	1.119	0.839
	$2^1B_u^-$	0.120	2.176	0.366
12	$2^1A_g^-$	0.071	2.094	0.324
	$1^1B_u^+$	0.914	1.137	0.829
	$2^1B_u^-$	0.129	2.247	0.350

7924 | *Phys. Chem. Chem. Phys.*, 2025, **27**, 7916–7928

This journal is © the Owner Societies 2025

doubly excited configurations grows with the length of the chain for both the $2^1A_g^-$ and $2^1B_u^-$ states.

4. Conclusions

The relative position of the ionic $1^1B_u^+$ excited state in polyenes is strongly influenced by the level of theory employed due to the more sensitive nature of this state with respect to electron correlation and orbital relaxation effects. Thus, a proper description of ionic states requires a combination of factors at the variational MR-CISD and MR-AQCC levels. Polarization through enhanced σ–π electron correlation significantly stabilizes the ionic state, whereas covalent states are already well described with an adequate treatment of non-dynamic correlation involving valence π-orbitals. Expanding the basis set to include larger polarization shells further stabilizes the ionic state but has minimal effect on covalent states. Additionally, size-extensivity corrections play a crucial role in stabilizing the ionic state. Therefore, an accurate description of the ionic state requires extensive treatment of σ–π electron correlation, a sufficiently large basis set, and the inclusion of size-extensivity corrections.

Based on these considerations, MR-CISD+P and MR-AQCC provide mutually consistent predictions that the $1^1B_u^+$ state is the first excited state in hexatriene and octatetraene. These findings align with theoretical reference benchmark values. For decapentaene, extrapolated MR-CISD+P results suggest that the $2^1A_g^-$ and $1^1B_u^+$ states are nearly degenerate, while MR-AQCC indicates that the ionic state lies approximately 0.2 eV below the covalent state. For dodecahexaene, the high computational cost associated with using an appropriate basis set precluded an accurate assignment of the ordering of the two low-lying states. However, our findings using the cc-pVDZ basis set suggest that the covalent $2^1A_g^-$ state is the lowest excited state, lying 0.2 eV below the ionic state at the MR-CISD+P level, while MR-AQCC results suggest that these states are virtually degenerate. The triplet states $1^3A_g^-$ and $1^3B_u^-$ are already well-described at the CASSCF level and can be reliably calculated using MR-CISD, MR-AQCC, or CASPT2.

Wavefunction analysis further revealed how the character of the wavefunctions evolves across the series in terms of ionic character, multiconfigurational character, and single-excitation character. The ionic state remains consistently well-represented by a single HOMO–LUMO excitation, whereas the contribution of doubly excited configurations increases with chain length for both covalent states. Notably, the $2^1B_u^-$ state exhibits an increasingly multiconfigurational character as the chain lengthens.

Data availability

The data supporting this article have been included as part of the ESI.†

Conflicts of interest

There are no conflicts to declare.

Acknowledgements

References

1 R. van Grondelle, J. P. Dekker, T. Gillbro and V. Sundstrom, Energy Transfer and Trapping in Photosynthesis, *Biochim. Biophys. Acta, Bioenerg.*, 1994, **1187**, 1–65.

2 H. van Amerongen and R. van Grondelle, Understanding the Energy Transfer Function of LHCII, the Major Light-Harvesting Complex of Green Plants, *J. Phys. Chem. B*, 2001, **105**, 604–617.

3 P. Horton, A. V. Ruban and R. G. Walters, Regulation of light harvesting in green plants, *Annu. Rev. Plant Physiol. Plant Mol. Biol.*, 1996, **47**, 655–684.

4 K. K. Niyogi, Photoprotection revisited: Genetic and Molecular Approaches, *Annu. Rev. Plant Physiol. Plant Mol. Biol.*, 1999, **50**, 333–359.

5 A. V. Ruban, R. Berera, C. Ilioaia, I. H. M. van Stokkum, J. T. M. Kennis, A. A. Pascal, H. van Amerongen, B. Robert, P. Horton and R. van Grondelle, Identification of a Mechanism of Photoprotective Energy Dissipation in Higher Plants, *Nature*, 2007, **450**, 575–578.

6 T. Yanai, Y. Kurashige, E. Neuscamman and G. K.-L. Chan, Multireference Quantum Chemistry through a Joint Density Matrix Renormalization Group and Canonical Transformation Theory, *J. Chem. Phys.*, 2010, 132.

7 V. Sauri, L. Serrano-Andrés, A. R. M. Shahi, L. Gagliardi, S. Vancoillie and K. Pierloot, Multiconfigurational Second-Order Perturbation Theory Restricted Active Space (RASPT2) Method for Electronic Excited States: A Benchmark Study, *J. Chem. Theory Comput.*, 2011, **7**, 153–168.

8 J. B. Schriber and F. A. Evangelista, Adaptive Configuration Interaction for Computing Challenging Electronic Excited States with Tunable Accuracy, *J. Chem. Theory Comput.*, 2017, **13**, 5354–5366.

9 T. Müller, M. Dallos and H. Lischka, The Ethylene $1\,^1B_{1u}$ V State Revisited, *J. Chem. Phys.*, 1999, **110**, 7176–7184.

This journal is © the Owner Societies 2025

Phys. Chem. Chem. Phys., 2025, **27**, 7916–7928 | 7925

10 M. Dallos and H. Lischka, A Systematic Theoretical Investigation of the Lowest Valence- and Rydberg-Excited Singlet States of Trans-Butadiene. The Character of the $1^1B_u(V)$ State Revisited, *Theor. Chem. Acc.*, 2004, **112**, 16–26.

11 A. Yu Sokolov, S. Guo, E. Ronca and G. K.-L. Chan, Time-Dependent N-Electron Valence Perturbation Theory with Matrix Product State Reference Wavefunctions for Large Active Spaces and Basis Sets: Applications to the Chromium Dimer and All-Trans Polyenes, *J. Chem. Phys.*, 2017, **146**.

12 P. K. Samanta, D. Mukherjee, M. Hanauer and A. Köhn, Excited States with Internally Contracted Multireference Coupled-Cluster Linear Response Theory, *J. Chem. Phys.*, 2014, **140**.

13 J. Gu, W. Wu, D. Danovich, R. Hoffmann, Y. Tsuji and S. Shaik, Valence Bond Theory Reveals Hidden Delocalized Diradical Character of Polyenes, *J. Am. Chem. Soc.*, 2017, **139**, 9302–9316.

14 C. M. Marian and N. Gilka, Performance of the Density Functional Theory/Multireference Configuration Interaction Method on Electronic Excitation of Extended π-Systems, *J. Chem. Theory Comput.*, 2008, **4**, 1501–1515.

15 D. Khokhlov and A. Belov, Toward an Accurate Ab Initio Description of Low-Lying Singlet Excited States of Polyenes, *J. Chem. Theory Comput.*, 2021, **17**, 4301–4315.

16 Z. Lu and S. Matsika, High-Multiplicity Natural Orbitals in Multireference Configuration Interaction for Excited States, *J. Chem. Theory Comput.*, 2012, **8**, 509–517.

17 M. T. do Casal, J. M. Toldo, F. Plasser and M. Barbatti, Using Diketopyrrolopyrroles to Stabilize Double Excitation and Control Internal Conversion, *Phys. Chem. Chem. Phys.*, 2022, **24**, 23279–23288.

18 A. V. Girija, W. Zeng, W. K. Myers, R. C. Kilbride, D. T. W. Toolan, C. Zhong, F. Plasser, A. Rao and H. Bronstein, Singlet Fission in Pechmann Dyes: Planar Chromophore Design and Understanding, *J. Am. Chem. Soc.*, 2024, **146**, 18253–18261.

19 P. Wang, R. Nakamura, Y. Kanematsu, Y. Koyama, H. Nagae, T. Nishio, H. Hashimoto and J.-P. Zhang, Low-Lying Singlet States of Carotenoids Having 8–13 Conjugated Double Bonds as Determined by Electronic Absorption Spectroscopy, *Chem. Phys. Lett.*, 2005, **410**, 108–114.

20 R. L. Christensen, M. G. I. Galinato, E. F. Chu, J. N. Howard, R. D. Broene and H. A. Frank, Energies of Low-Lying Excited States of Linear Polyenes, *J. Phys. Chem. A*, 2008, **112**, 12629–12636.

21 R. M. Gavin, S. Risemberg and S. A. Rice, Spectroscopic Properties of Polyenes. I. The Lowest Energy Allowed Singlet-Singlet Transition for *Cis*- and *Trans*-1,3,5-Hexatriene, *J. Chem. Phys.*, 1973, **58**, 3160–3165.

22 R. M. Gavin, C. Weisman, J. K. McVey and S. A. Rice, Spectroscopic Properties of Polyenes. III. 1,3,5,7-Octatetraene, *J. Chem. Phys.*, 1978, **68**, 522–529.

23 K. L. D'Amico, C. Manos and R. L. Christensen, Electronic Energy Levels in a Homologous Series of Unsubstituted Linear Polyenes, *J. Am. Chem. Soc.*, 1980, **102**, 1777–1782.

24 M. Schmidt and P. Tavan, Electronic Excitations in Long Polyenes Revisited, *J. Chem. Phys.*, 2012, **136**, 124309.

25 D. Khokhlov and A. Belov, Ab Initio Study of Low-Lying Excited States of Carotenoid-Derived Polyenes, *J. Phys. Chem. A*, 2020, **124**, 5790–5803.

26 R. Guareschi and C. Angeli, The Lowest Singlet States of Hexatriene Revisited, *Theor. Chem. Acc.*, 2023, **142**, 127.

27 R. Pariser and R. G. Parr, A Semi-Empirical Theory of the Electronic Spectra and Electronic Structure of Complex Unsaturated Molecules. I, *J. Chem. Phys.*, 1953, **21**, 466–471.

28 R. Pariser and R. G. Parr, A Semi-Empirical Theory of the Electronic Spectra and Electronic Structure of Complex Unsaturated Molecules. II, *J. Chem. Phys.*, 1953, **21**, 767–776.

29 J. A. Pople, Electron Interaction in Unsaturated Hydrocarbons, *Trans. Faraday Soc.*, 1953, **49**, 1375.

30 K. Schulten, I. Ohmine and M. Karplus, Correlation Effects in the Spectra of Polyenes, *J. Chem. Phys.*, 1976, **64**, 4422–4441.

31 P. Kimber and F. Plasser, Classification and Analysis of Molecular Excited States, *Comprehensive Computational Chemistry*, Elsevier, 2024, pp. 55–83.

32 M. T. do Casal, J. M. Toldo, M. Barbatti and F. Plasser, Classification of Doubly Excited Molecular Electronic States, *Chem. Sci.*, 2023, **14**, 4012–4026.

33 M. R. Silva-Junior, M. Schreiber, S. P. A. Sauer and W. Thiel, Benchmarks for Electronically Excited States: Time-Dependent Density Functional Theory and Density Functional Theory Based Multireference Configuration Interaction, *J. Chem. Phys.*, 2008, **129**, 104103.

34 C.-P. Hsu, S. Hirata and M. Head-Gordon, Excitation Energies from Time-Dependent Density Functional Theory for Linear Polyene Oligomers: Butadiene to Decapentaene, *J. Phys. Chem. A*, 2001, **105**, 451–458.

35 M. J. G. Peach, E. I. Tellgren, P. Sałek, T. Helgaker and D. J. Tozer, Structural and Electronic Properties of Polyacetylene and Polyyne from Hybrid and Coulomb-Attenuated Density Functionals, *J. Phys. Chem. A*, 2007, **111**, 11930–11935.

36 J. H. Starcke, M. Wormit, J. Schirmer and A. Dreuw, How Much Double Excitation Character Do the Lowest Excited States of Linear Polyenes Have?, *Chem. Phys.*, 2006, **329**, 39–49.

37 K. Boguslawski, Targeting Excited States in All-Trans Polyenes with Electron-Pair States, *J. Chem. Phys.*, 2016, **145**, 234105.

38 S. A. do Monte, R. F. K. Spada, R. L. R. Alves, L. Belcher, R. Shepard, H. Lischka and F. Plasser, Quantification of the Ionic Character of Multiconfigurational Wave Functions: The Q_a^t Diagnostic, *J. Phys. Chem. A*, 2023, **127**, 9842–9852.

39 M. Boggio-Pasqua, M. J. Bearpark, M. Klene and M. A. Robb, A Computational Strategy for Geometry Optimization of Ionic and Covalent Excited States, Applied to Butadiene and Hexatriene, *J. Chem. Phys.*, 2004, **120**, 7849–7860.

40 C. Angeli, On the Nature of the π → π* Ionic Excited States: The V State of Ethene as a Prototype, *J. Comput. Chem.*, 2009, **30**, 1319–1333.

41 C. Angeli and M. Pastore, The Lowest Singlet States of Octatetraene Revisited, *J. Chem. Phys.*, 2011, **134**, 184302.

7926 | *Phys. Chem. Chem. Phys.*, 2025, **27**, 7916–7928

This journal is © the Owner Societies 2025

42 T. Tran, J. Segarra-Martí, M. J. Bearpark and M. A. Robb, Molecular Vertical Excitation Energies Studied with First-Order RASSCF (RAS[1,1]): Balancing Covalent and Ionic Excited States, *J. Phys. Chem. A*, 2019, **123**, 5223–5230.

43 H. Lischka, D. Nachtigallová, A. J. A. Aquino, P. G. Szalay, F. Plasser, F. B. C. Machado and M. Barbatti, Multireference Approaches for Excited States of Molecules, *Chem. Rev.*, 2018, **118**, 7293–7361.

44 K. Nakayama, H. Nakano and K. Hirao, Theoretical Study of the $\pi \rightarrow \pi^*$ Excited States of Linear Polyenes: The Energy Gap between $1^1B_u^+$ and $2^1A_g^-$ States and Their Character, *Int. J. Quantum Chem.*, 1998, **66**, 157–175.

45 L. Serrano-Andrés, M. Merchán, I. Nebot-Gil, R. Lindh and B. O. Roos, Towards an Accurate Molecular Orbital Theory for Excited States: Ethene, Butadiene, and Hexatriene, *J. Chem. Phys.*, 1993, **98**, 3151–3162.

46 L. Serrano-Andres, R. Lindh, B. O. Roos and M. Merchan, Theoretical Study of the Electronic Spectrum of All-*Trans*-1,3,5,7-Octatetraene, *J. Chem. Phys.*, 1993, **97**, 9360–9368.

47 M. Schreiber, M. R. Silva-Junior, S. P. A. Sauer and W. Thiel, Benchmarks for Electronically Excited States: CASPT2, CC2, CCSD, and CC3, *J. Chem. Phys.*, 2008, **128**, 134110.

48 M. Véril, A. Scemama, M. Caffarel, F. Lipparini, M. Boggio-Pasqua, D. Jacquemin and P. Loos, QUESTDB: A Database of Highly Accurate Excitation Energies for the Electronic Structure Community, *Wiley Interdiscip. Rev.: Comput. Mol. Sci.*, 2021, **11**, e1517.

49 P. G. Szalay, T. Müller, G. Gidofalvi, H. Lischka and R. Shepard, Multiconfiguration Self-Consistent Field and Multireference Configuration Interaction Methods and Applications, *Chem. Rev.*, 2012, **112**, 108–181.

50 P. G. Szalay and R. J. Bartlett, Multi-Reference Averaged Quadratic Coupled-Cluster Method: A Size-Extensive Modification of Multi-Reference CI, *Chem. Phys. Lett.*, 1993, **214**, 481–488.

51 P. G. Szalay and R. J. Bartlett, Approximately Extensive Modifications of the Multireference Configuration Interaction Method: A Theoretical and Practical Analysis, *J. Chem. Phys.*, 1995, **103**, 3600–3612.

52 H. Lischka, R. Shepard, R. M. Pitzer, I. Shavitt, M. Dallos, T. Müller, P. G. Szalay, M. Seth, G. S. Kedziora, S. Yabushita and Z. Zhang, High-Level Multireference Methods in the Quantum-Chemistry Program System COLUMBUS: Analytic MR-CISD and MR-AQCC Gradients and MR-AQCC-LRT for Excited States, GUGA Spin–Orbit CI and Parallel CI Density, *Phys. Chem. Chem. Phys.*, 2001, **3**, 664–673.

53 P. G. Szalay, T. Müller and H. Lischka, Excitation Energies and Transition Moments by the Multireference Averaged Quadratic Coupled Cluster (MR-AQCC) Method, *Phys. Chem. Chem. Phys.*, 2000, **2**, 2067–2073.

54 J.-D. Chai and M. Head-Gordon, Long-Range Corrected Hybrid Density Functionals with Damped Atom–Atom Dispersion Corrections, *Phys. Chem. Chem. Phys.*, 2008, **10**, 6615.

55 T. H. Dunning, Gaussian Basis Sets for Use in Correlated Molecular Calculations. I. The Atoms Boron through Neon and Hydrogen, *J. Chem. Phys.*, 1989, **90**, 1007–1023.

56 B. O. Roos, P. R. Taylor and P. E. M. Sigbahn, A Complete Active Space SCF Method (CASSCF) Using a Density Matrix Formulated Super-CI Approach, *Chem. Phys.*, 1980, **48**, 157–173.

57 J. A. Pople, R. Seeger and R. Krishnan, Variational Configuration Interaction Methods and Comparison with Perturbation Theory, *Int. J. Quantum Chem.*, 2009, **12**, 149–163.

58 A. Bunge, Electronic Wavefunctions for Atoms. III. Partition of Degenerate Spaces and Ground State of C, *J. Chem. Phys.*, 1970, **53**, 20–28.

59 A. Halkier, T. Helgaker, P. Jørgensen, W. Klopper, H. Koch, J. Olsen and A. K. Wilson, Basis-Set Convergence in Correlated Calculations on Ne, N_2, and H_2O, *Chem. Phys. Lett.*, 1998, **286**, 243–252.

60 K. Andersson, P. A. Malmqvist, B. O. Roos, A. J. Sadlej and K. Wolinski, Second-Order Perturbation Theory with a CASSCF Reference Function, *J. Phys. Chem.*, 1990, **94**, 5483–5488.

61 M. J. Frisch, G. W. Trucks and H. B. Schlegel, *et al.*, *Gaussian 16 Revision C.01*, 2016.

62 H. Lischka, T. Müller, P. G. Szalay, I. Shavitt, R. M. Pitzer and R. Shepard, COLUMBUS—a Program System for Advanced Multireference Theory Calculations, *Wiley Interdiscip. Rev.: Comput. Mol. Sci.*, 2011, **1**, 191–199.

63 H. Lischka, R. Shepard and T. Müller, *et al.*, The Generality of the GUGA MRCI Approach in COLUMBUS for Treating Complex Quantum Chemistry, *J. Chem. Phys.*, 2020, **152**, 134110.

64 T. Helgaker, H. J. A. Jensen and P. Jorgensen, *et al.*, *DALTON, an Ab Initio Electronic Structure Program, Release 1.0*, 1997.

65 G. Li Manni, I. F. Galván and A. Alavi, *et al.*, The Open-Molcas Web: A Community-Driven Approach to Advancing Computational Chemistry, *J. Chem. Theory Comput.*, 2023, **19**, 6933–6991.

66 P.-O. Löwdin, On the Non-Orthogonality Problem Connected with the Use of Atomic Wave Functions in the Theory of Molecules and Crystals, *J. Chem. Phys.*, 1950, **18**, 365–375.

67 F. Plasser and H. Lischka, Analysis of Excitonic and Charge Transfer Interactions from Quantum Chemical Calculations, *J. Chem. Theory Comput.*, 2012, **8**, 2777–2789.

68 F. Plasser, Entanglement Entropy of Electronic Excitations, *J. Chem. Phys.*, 2016, **144**, 194107.

69 F. Plasser, M. Wormit and A. Dreuw, New Tools for the Systematic Analysis and Visualization of Electronic Excitations. I. Formalism, *J. Chem. Phys.*, 2014, **141**, 024106.

70 S. Matsika, X. Feng, A. V. Luzanov and A. I. Krylov, What We Can Learn from the Norms of One-Particle Density Matrices, and What We Can't: Some Results for Interstate Properties in Model Singlet Fission Systems, *J. Phys. Chem. A*, 2014, **118**, 11943–11955.

71 P. Kimber and F. Plasser, Toward an Understanding of Electronic Excitation Energies beyond the Molecular Orbital Picture, *Phys. Chem. Chem. Phys.*, 2020, **22**, 6058–6080.

72 F. Plasser, TheoDORE: A Toolbox for a Detailed and Automated Analysis of Electronic Excited State Computations, *J. Chem. Phys.*, 2020, **152**, 084108.

73 F. Kossoski, M. Boggio-Pasqua, P.-F. Loos and D. Jacquemin, Reference Energies for Double Excitations: Improvement and Extension, *J. Chem. Theory Comput.*, 2024, **20**, 5655–5678.

This journal is © the Owner Societies 2025

Phys. Chem. Chem. Phys., 2025, **27**, 7916–7928 | **7927**

74 M. F. S. J. Menger and H. Köppel, On the Fluorescence Properties and Nonradiative Transitions in Medium-Sized All-Trans Polyenes, *J. Phys. Chem. A*, 2023, **127**, 8501–8507.

75 M. Barbatti, A. J. A. Aquino and H. Lischka, The UV Absorption of Nucleobases: Semi-Classical Ab Initio Spectra Simulations, *Phys. Chem. Chem. Phys.*, 2010, **12**, 4959.

76 R. M. Gavin and S. A. Rice, Spectroscopic Properties of Polyenes. II. The Vacuum Ultraviolet Spectra of *Cis-* and *Trans-*1,3,5-Hexatriene, *J. Chem. Phys.*, 1974, **60**, 3231–3237.

77 D. G. Leopold, V. Vaida and M. F. Granville, Direct Absorption Spectroscopy of Jet-Cooled Polyenes. I. The $1^1B_u^+ \leftarrow 1^1A_g^-$ Transition of trans,trans-1,3,5,7-Octatetraene, *J. Chem. Phys.*, 1984, **81**, 4210–4217.

78 D. G. Leopold, R. D. Pendley, J. L. Roebber, R. J. Hemley and V. Vaida, Direct Absorption Spectroscopy of Jet-Cooled Polyenes. II. The $1^1B_u^+ \leftarrow 1^1A_g^-$ Transitions of Butadienes and Hexatrienes, *J. Chem. Phys.*, 1984, **81**, 4218–4229.

79 L. A. Heimbrook, B. E. Kohler and I. J. Levy, Fluorescence from the 1^1B_u State of trans,trans-1,3,5,7-Octatetraene in a Free Jet, *J. Chem. Phys.*, 1984, **81**, 1592–1597.

80 H. Petek, A. J. Bell, Y. S. Choi, K. Yoshihara, B. A. Tounge and R. L. Christensen, The 2^1A_g State of trans,trans -1,3,5,7-Octatetraene in Free Jet Expansions, *J. Chem. Phys.*, 1993, **98**, 3777–3794.

81 W. M. Flicker, O. A. Mosher and A. Kuppermann, Low Energy, Variable Angle Electron-Impact Excitation of 1,3,5-Hexatriene, *Chem. Phys. Lett.*, 1977, **45**, 492–497.

82 M. Allan, L. Neuhaus and E. Haselbach, All-E-1,3,5,7-Octatetraene: Electron-Energy-Loss and Electron-Transmission Spectra, *Helv. Chim. Acta*, 1984, **67**, 1776–1782.

83 Z. Yang, Z. Mao, Z. Xie, Y. Zhang, S. Liu, J. Zhao, J. Xu, Z. Chi and M. P. Aldred, Recent Advances in Organic Thermally Activated Delayed Fluorescence Materials, *Chem. Soc. Rev.*, 2017, **46**, 915–1016.

84 F. B. Dias, T. J. Penfold and A. P. Monkman, Photophysics of Thermally Activated Delayed Fluorescence Molecules, *Methods Appl. Fluoresc.*, 2017, **5**, 012001.

85 P. Kimber and F. Plasser, Energy Component Analysis for Electronically Excited States of Molecules: Why the Lowest Excited State Is Not Always the HOMO/LUMO Transition, *J. Chem. Theory Comput.*, 2023, **19**, 2340–2352.